# Bayesian based Damage Segmentation for Structural Health Monitoring

G. Li[1], F. G. Yuan[1*], R. T. Haftka[2] and N. H. Kim[2]

[1]Department of Mechanical and Aerospace Engineering,

North Carolina State University, Raleigh, NC, 27695, USA

[2]Department of Mechanical and Aerospace Engineering,

University of Florida, Gainesville, FL 32611, USA

*Email: yuan@ncsu.edu

**Abstract**

A segmentation technique based on Bayesian updating framework is developed for structural damage diagnosis in the context of structural health monitoring (SHM). This probabilistic framework enables taking into account the prior information such as spatial constraints and image smoothness in the segmentation process. Markov random field is employed to model the *prior* due to the spatial constraint in the neighboring SHM images. Results show that the Bayesian segmentation method has potential to differentiate damage region from the background for SHM images. Compared to the ad-hoc *k*-means clustering method, it yields more accurate damage sizes automatically than by eliminating random noises and inhibiting fuzzy edges.

**Keywords**: Damage Segmentation, Damage Sizing, Damage Diagnostics, Bayesian Updating, Structural Health Monitoring.

## 1. Introduction

Most engineering materials and structures contain micro-defects due to the imperfection of manufacturing [1]. Micro-defects will nucleate and form macro-defects, e.g. cracks, after many fatigue loading cycles. Structural components with macro-defects or damage do not need to be replaced before the damage reaches a critical size. Early stage diagnosis is essential for subsequent structural prognosis and health management (PHM) in estimating the remaining useful life (RUL) of the structure. Diagnosis is to determine the current status of the structures, while prognosis is to predict its future status, and confident prognosis is based on accurate diagnosis.

Visual images that portray the location, size, and shape of the damage provide a direct intuitive way to reflect the condition of structures. Recently, damage imaging has been developed for monitoring plate-like structures with a pre-installed sensor array. The imaging results provide not only evidence on damage existence but also the quantitative information of damage size and location. In previous research, Lin and Yuan [2-3] employed a migration technique originating from seismic imaging to detect point-like and circular-shaped damage on aluminum plates. Wang and Yuan [4] extended the migration technique to composite plates. Zhao *et al.* [5] developed a computed tomography imaging algorithm, which is based on calculating the difference coefficient of the signals between the damaged and

pristine structures. Sicard *et al.*[6] employed a synthetic aperture focusing technique (SAFT) for damage imaging on isotropic plate structures. Liu and Hong [7] applied a sixteen-element piezoelectric phased array to image the damage in a three dimensional space. Wang *et al.* [8] developed an imaging algorithm based on the time reversal concept of wave propagation for distributed sensor arrays. In spite of different degrees of image resolution and accuracy of these methods, the imaging results provide a two-dimensional damage distribution map, in which the pixel value of each location represents the severity of damage. Thus the distribution not only reflects the existence but also the shape and severity of damage.

The objective of this study is to separate the damaged region in SHM images and obtain more accurate estimation of crack size. The image segmentation used in the medical imaging[9] is applied to segment the damaged region from the damage distribution map that can be obtained from various damage imaging algorithms. This segmentation procedure is robust against noise and allows eliminating fuzzy edges. An imaging algorithm employed in this study is a migration technique developed in a previous study [2] because it provides clear images reflecting the damage in structures. The appearance of the image provides a gross indication of the damage state, yet it is not less quantifiable to determine the damaged region. While damage imaging algorithms have been investigated [2, 8, 10-11], knowledge extraction from damage images remains elusive. Zhao *et al.* [5] used a thresholding method to segment the damaged region from its background. In this paper, without a threshold, a damage segmentation method in the context of Bayesian framework with Markov random field (MRF) is developed for discerning the damage region from the background. Images generated from the migration technique are contaminated with simulated random noises to simulate testing noise in environments.

The remaining of the paper is organized as the following. Section 2 introduces the basic concept of image segmentation, and reviews frequently used segmentation algorithms. Section 3 introduces the theory of Bayesian updating for the purpose of damage segmentation. Section 4 defines the prior knowledge, MRF, for the image segmentation. Section 5 deduces the formulation of mathematical model for the image segmentation under the Bayesian framework, and achieves the damage segmentation result with maximizing a posterior (MAP) criterion. Section 6 briefly introduces an f-k migration technique and applies the Bayesian image segmentation method to an f-k migration image. The effect of prior information in the whole image segmentation procedure is investigated. Cracks located at different positions are used to validate the robustness of the Bayesian based damage segmentation method. Further accuracy enhancement is achieved by carrying out multiple-frequency excitation in Bayesian framework. Section 7 provides concluding remarks.

## 2. Image segmentation

Image segmentation refers to the process of partitioning an image into multiple regions with different class labels. The goal of segmentation is to simplify an image into several divisions (classes), each of which possesses distinct attributes. Figure 1 shows illustrative image intensity (a) in grey scale and a possible segmentation (b) into two classes, in which Class 1 is separated as an object from the background (Class 2). Although well-trained human naked eyes with experience can identify the segmented regions from the original images, it is a daunting task for a computer to automatically divide an observed image into meaningful regions, especially when it is contaminated by noise. Researchers have developed many methods based on clustering concepts such as *k*-means clustering [12], fuzzy mathematics, neural network, and statistical models [13-15]. Bayesian based segmentation is a viable approach [16], which takes advantage of a statistical model to combine the current observed data with prior knowledge, such as spatial constraints and smoothness level.

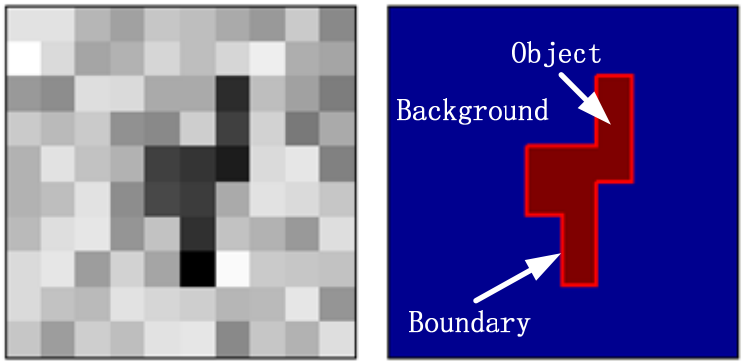


Figure 1. Illustrative example of image segmentation, (a) Image intensity and (b) its binary segmentation

The segmentation technique based on Bayesian updating has been successfully applied in several fields including medical image analysis [17-18], satellite image analysis, and computer vision [19-20]. For the application of identifying damaged region, this technique primarily aims at segmenting out the damaged region(s) from a damage distribution map provided by image pixels. In the Bayesian updating procedure for image segmentation, the prior can represent any information available to the analyst. The first type of prior information used in this paper is the fact that the size of pixels is small compared to that of damage. Consequently, if a pixel is in the damaged region, the probability of neighboring pixels to be in the damaged region is higher than for other pixels. This property is represented here by a Markov random field (MRF) [Reference here], which describes the relationship between the neighboring pixels. With the MRF, the segmented labels tend to be the same as its neighbors. As a result, the imaged pixels of damaged regions are highlighted, the noise is eliminated, and the fuzzy tails (Refer to Figure 5) which are caused by the limited number of sensors and may lead to faulty estimation of damage size, could be well suppressed.

## 3. Bayesian updating

Bayesian updating is statistical inference in which evidence or observations are used to update or to newly infer the probability that a hypothesis may be true. It uses aspects of the scientific inference, which involves collecting evidence that is meant to be consistent or inconsistent with a given hypothesis. When the collected evidence is in accordance with the hypothesis, the hypothesis will be reinforced, on the other hand, if the collected evidence is not in conformity with the hypothesis, the hypothesis will be distorted or modify gradually to a new version. Therefore, as evidence accumulates, the degree of belief in a hypothesis will change.

Bayesian theorem [21] relates the posterior probability density function (PDF) to the likelihood function and the prior function (a marginal PDF) in a form as,

$$p(x \mid y) = \frac{p(y \mid x)p(x)}{p(y)} \tag{1}$$

in which $p(x)$ is the prior PDF of event $x$ before the observation. It is 'prior' in the sense that it does not take into account any information about the current observation $y$. $p(x \mid y)$ is a conditional PDF of $x$ after the observation, given new data $y$. In Bayesian statistics, it is the posterior PDF because it is inferred from the prior and observed data.

$p(y \mid x)$ is a likelihood function, which is the conditional PDF of $y$ given $x$. $p(y)$ is a marginal PDF for normalization.

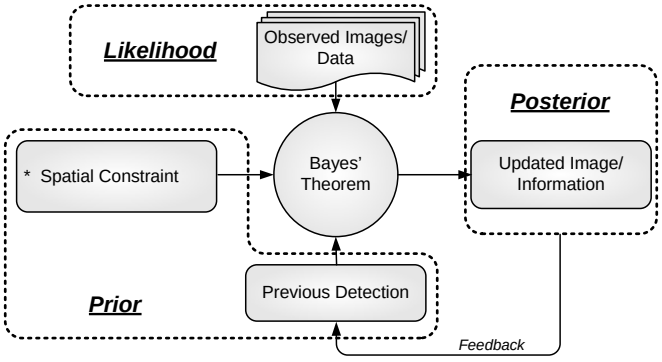


Figure 2. Bayesian updating framework for segmentation

In damage segmentation, the prior PDF $p(x)$ represents prior information about the SHM images. For instance, the assumption includes a spatial constraint on pixels, correlation among pixels, noise level in measurement environments, images from other SHM system, geometry or boundary conditions of the structure, and previous detected damage images. The likelihood function represents the observed information, which is the pixel value of the detected image intensity. Figure 2 shows the Bayesian updating framework for damage segmentation. In this paper, the spatial constraint, which is described by MRF, will be considered as prior. The Bayesian updating framework for other types of priors is similar to that of the spatial constraint.

## 4. Prior model

In the SHM image segmentation, the relationship between pixels in the grid is emphasized. Markov random field is employed to model the correlation between neighboring pixels. MRF image modeling has been used successfully in many image processing applications[22-24]. The success of MRF modeling mainly arises from its systematic and flexible treatment of the contextual information in the image and prior knowledge for the segmentation procedure can be easily quantified by MRF model parameters [19, 25]. Image segmentation processes the property of contextual smoothness of the class labels in the image space so that a pixel with a particular class label is likely to share the label with its immediate neighbors. Moreover a Bayesian framework using spatial local MRF make the segmentation procedure computational feasible [20]. Following are some basic definitions and derivations for the image segmentation based on Bayesian updating framework with MRF prior.

### *4.1 Neighborhood*

In image processing, a neighborhood system $\eta$ associated with the whole image domain $\Omega$ is a collection of neighborhoods, where each neighborhood of the pixel at the site of $s$ satisfying following two conditions.

(1) The pixel $s$ does not belong to its own neighborhood;

(2) The pixel $s$ belonging to the neighborhood of pixel $t$ implies that pixel $t$ belongs to the neighborhood of pixel $s$.

### *4.2 Cliques in neighborhood*

Considering an image defined on a Cartesian coordinate, a clique is a subset $C$ of the whole image $\Omega$ if two different elements of C are neighbors. Figure 3 gives the second-order neighborhood [25], all the available cliques, and several illustrative non-clique pixels in this 8-element neighboring system. The definition of clique system makes the neighboring pixels correlated with each other.

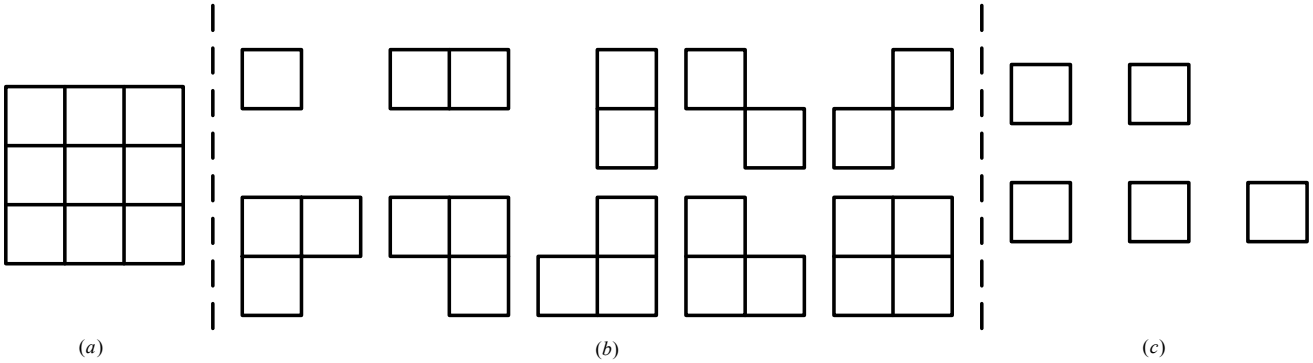


Figure 3 Illustration of cliques in the second-order neighborhood, (a)2nd order neighborhood and (b) its cliques and (c) non-cliques

*4.3 Markov Random Field*

A Markov random field (MRF) on ($\Omega$, $\eta$) is a random field with its probability property of each pixel in the whole field satisfying the Markovian property described as following two equations,

$$p(X = x) \geq 0 \text{ for all } x \in \Omega \tag{2}$$

$$p(X_s = x_s \mid X_t = x_t, \forall t \in \Omega, t \neq s) = p(X_s = x_s \mid X_t = x_t, t \in \eta_s), \forall t, s \in \Omega \tag{3}$$

where $\Omega$ represent the whole image domain, $\eta$ is the predefined neighboring system formulation of $s$ (In this paper, the 8-element second order neighboring system is used due to computational complexity). $s$ is the evaluated pixel/site, $\eta_s$ is the neighboring system of $s$. $X_s$ is the event which cluster the evaluated pixel should be, and the $x_s$ is the possible cluster value(in damage segmentation, it may be a Boolean variable 0 or 1, which indicate undamaged or damaged) of the evaluated pixel. $p(\cdot)$ is the PDF of events stated in the bracket. Eq. (2) indicates that in all the configuration space the labeling procedure assigns a positive probability to all the images in the configuration space. Eq. (3) shows that when labeling a pixel, the probability of the label given all the labels in the whole image equals to the probability of label given the labels in its neighborhood. Thus, MRF is locally dependent random field.

*4.4 Gibbs Random Field*

A random field $X$ with ($\Omega$, $\eta$, $C$), is a Gibbs random field (GRF) if its distribution has the following form[25],

$$p(x) = \frac{1}{Z} e^{\left(\sum_{c \in C} V_c(x)\right)} \tag{4}$$

where $C$ is the set of all cliques in $\Omega$, $Z$ is the normalizing constant, and $V_c(x)$ is the clique potential associated with clique $c$. There is no particular restriction on the clique potential definition. As long as the resulting Gibbs distribution satisfies the definition of the probability, the associated clique potentials are valid. The Gibbs potential can be defined such that some specific features of the image can be identified and emphasized. In addition, it is not necessary to use all types of cliques for a given neighborhood system; that is, specific set of clique types can be selectively used for specific problems, such as texture image segmentation.

Prior knowledge of the Bayesian based image segmentation, e.g. the spatial constraint on the class label, can be incorporated into the Gibbs distribution by the choice of specific clique types and their potentials. The smoothness of

the class label in image space can be measured by defining the clique potential such that a high positive clique potential is assigned only when all class label in the clique are identical.

### *4.5 Hammersley-Clifford Theorem*

Hammersley-Clifford Theorem [25] builds a bridge between MRF and GRF. It indicates that a random field *X,* on (Ω, $\eta$, *C*), is a MRF with respect to $\eta$ if and only if $p(x)$ has a Gibbs distribution with respect to $\eta$. Thus, it is possible to express the conditional probability of a MRF in terms of clique potentials. This is useful in practice because it is easy to choose the clique types and their potentials to describe the desired local behavior. For example, spatial relationships such as smoothness and continuity of the neighboring pixels can be specified by clique potential $\beta$. It is crucial for the theorem to share the same neighborhood system $\eta$ and the associate clique $c$ for both MRF and GRF.

The SHM image is constructed by the pixels in the square lattices, which is considered as a MRF as described above for its close-neighboring correlation. Those damage areas are with high grey level pixels in its lattice. Through the GRF, which reflects the property of MRF and has concrete representation – Gibbs potential, this information will be transmitted to the probability of damage, which will affect the determination of whether the pixel belong to the damaged class or undamaged class. The prior density represents the strength of correlation between the pixels in cliques through the formulation of Gibbs potential.

## 5. Formulation for damage segmentation

The damage image created by the signals from sensor array is usually noisy and with fuzzy tails due to measurement environment and the limited number of sensors. The image is composed of small lattice blocks, in which correlative potential is preset with the form of MRF. In the crack contained images, noise can be canceled and fuzzy tails can be suppressed by assigning those pixels with similar neighbors to a high probability and those pixels with different neighbors to a low probability. Thus, the segmentation procedure depends not only on the detected image intensity but also on the spatial relation with the neighboring system.

The maximum a posteriori (MAP) criterion [26] is used in this paper to make a decision for problems which need to include the prior knowledge and current observation. According to the MAP criterion, given a realization of a random field, the goal is to find an optimal realization of $\hat{x}$, which maximizes the a posteriori probability $p(x \mid y)$ for all possible realizations of *x*. The maximization procedure can be equivalently expressed as:

$$\hat{x} = \arg\max_{x} \left\{ \sum_{\Omega} p(x \mid y) \right\} \tag{5}$$

where argmax is an operation to achieve estimation of the given argument for which the value of the given expression attains its maximum value.

The image segmentation problem can be achieved by estimating $\hat{x}$ though maximize the posterior conditional probability function, $p(x \mid y)$, which indicate the probability of the pixel belong to a specific segmentation class $x$ given the current observation $y$. Substitute Eq. (1) into Eq. (5), the estimation of *x* can be rewrite as,

$$\hat{x} = \arg\max_{x} \left\{ \sum_{\Omega} \frac{p(y \mid x) p(x)}{p(y)} \right\} \tag{6}$$

Since the marginal probability $p(y)$ is a normalization item, which will not affect the affect the comparison of probability of the observed pixel belonging to a given class. Therefore, for the purpose of pixel classification, Eq. (6) can be simplified.

$$\hat{x} = \arg\max_{x} \left\{ \sum_{\Omega} p(y \mid x) p(x) \right\} \tag{7}$$

In Eq.(7), the estimation of class for each pixel are determined by two factors, $p(x)$ and $p(y \mid x)$. $p(x)$ is the prior information, which in the image segmentation problem is the assumed segmentation class label. $p(y \mid x)$ is the observed information, which indicate the probability of the pixel equal to the observed value given the pixel belonging to a specific class. Equivalently, the estimation of $x$ can be achieved by maximizing the natural logarithm of the posterior,

$$\hat{x} = \arg\max_{x} \left\{ \sum_{\Omega} \ln p(y \mid x) + \ln p(x) \right\} \tag{8}$$

Gaussian distribution [20], as in Eq. (9), is employed to model the likelihood, which represents the noise-polluted SHM images. The intensity of the region is modeled as a signal $\mu_s$ plus white Gaussian noise with variance $\sigma^2$.

$$p(y \mid x) = \frac{1}{\sqrt{2\pi\sigma^2}} e^{\left( -\frac{1}{2\sigma^2} \left( y_s - \mu_s^{x_s} \right)^2 \right)} \tag{9}$$

where $s$ indicates the location of pixel. The superscript $x_s$ of $\mu_s$ is index, not an exponent. Substitute Eq. (4) and Eq. (9) into Eq. (8), the segmentation problem can finally be described as in Eq. (10).

$$p(x \mid y) \propto e^{\left( -\sum_{\Omega} \frac{1}{2\sigma^2} \left[ y_s - \mu_s^{x_s} \right]^2 - \sum_{C} V_C(x) \right)} \tag{10}$$

where $x$ is the segmentation label ranging from 1 to $k$. $s$ is the position of the estimated grid. $y_s$ is the observed value (gray-value of segmented images). And $\mu_s$ is the mean value in the window with a certain size centered at the observed pixel $s$.

From Eq.(10), the posterior PDF is composed of two parts: Gaussian distribution likelihood and prior density function (Gibbs potential). The first part is essentially a $k$-means clustering algorithm, which calculates the distance between the evaluated pixel and the clustering center. If the evaluated pixel value is close to one cluster center, the posterior energy function will be enhanced. The second part is the adjustable part according to the Gibbs potential guided neighboring system. If the neighbor clique member is in the same label, then the Gibbs potential $V_c(x)$ should be negative, and the posterior energy density will be enhanced. On the other hand, if the clique members are at different labels, the posterior energy density will be weakened. For a specific case, neglecting the prior distribution by setting all $\beta$ as 0, this algorithm degenerates to a $k$-means clustering method which only counts the distance between each pixel with the clustering centers.

For computational efficiency, the 2nd-order clique is adopted, which contains an 8-element neighborhood as shown in Figure 3. According to the MRF-GRF equivalence described by Hammersley-Clifford theorem, the clique potential is given in the form of Gibbs density as in Eq. (2). The Gibbs potential value is defined as [20]

$$V_C(x) = \begin{cases} -\beta \text{ if } x_s = x_q \text{ and } s,q \in C \\ +\beta \text{ if } x_s \neq x_q \text{ and } s,q \in C \end{cases} \tag{11}$$

where $\beta$ is positive potential parameter, which reflect the possibility of a pixel being damaged if the neighboring pixel in the clique set is damaged. For example,

$$\beta = \{x_s = x_{damaged} \mid x_q = x_{damaged} \} \tag{12}$$

where, $x_{\text{damaged}}$ is the cluster label of damaged region. The choice of $\beta$ will affect strength of the spatial constraint in the GRF. Larger $\beta$ results in stronger spatial constraint; that is, neighbors are more likely to have the same label. This tendency will lead to the conservation of real damage area and cancellation of random noise area in the segmentation procedure for SHM images.

## 6. Application to SHM images

### *6.1 f-k migration imaging and its segmentation*

The f-k migration technique can effectively interpret the sensor data recorded by a distributed linear array sensor system and makes it possible to establish an active, in-service, and intelligent monitoring system. The image for segmentation is obtained from an active diagnostic linear array of actuators/sensors, which is used to excite/receive flexural waves[3]. The wave field scattered from the damage and sensor array data are synthesized using a two-dimensional explicit finite difference algorithm to model wave propagation in plates. The damage image can be represented by the cross-correlation in the frequency domain as

$$\mathbf{I}(x,y) = \sum\nolimits_{\omega} \mathbf{w}^{e*}(x,y,\omega)\,\mathbf{w}^{s}(x,y,\omega) \tag{13}$$

in which, **I** is the intensity matrix, and **I**($x$, $y$) is intensity value of each pixel at location with coordinate ($x$, $y$), $\mathbf{w}^{e*}$and $\mathbf{w}^{s}$ are the extrapolated excitation and scattered wave-fields[3] in frequency domain, respectively.

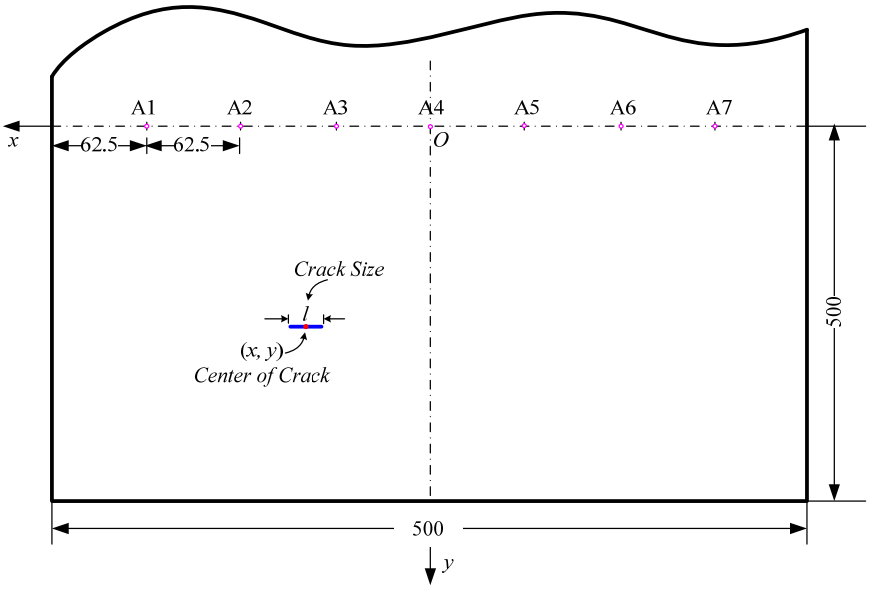


Figure 4. f-k migration simulation model

The numerical simulation is modeled as in Figure 4, in which the center of the crack is set at location ($x$, $y$) with crack size $l$ = 20mm, and the dots are A1~A7 are simulating piezoelectric transducers acting as both actuators and sensors. Mesh size of the f-k migration is 2.5mm.

Figure 5 (a) is a *f-k* migration imaging result polluted with random noise (the SNR of the image is 10dB, where the SNR is defined as in Eq. (14)) with a seven-sensor array for an aluminum plate structure using 150kHz excitation frequency.

$$SNR = 10\log_{10}\left(\frac{P_s}{P_n}\right) = 10\log_{10}\left(\frac{\sum_{i=1}^{m}\sum_{j=1}^{n} I_s^{\,2}}{\sum_{i=1}^{m}\sum_{j=1}^{n} I_n^{\,2}}\right) \tag{14}$$

where $P_s$ is the power of image intensity and $P_n$ is the power of image noise. $I_s$ is the intensity value of single and $I_n$ is the intensity value of noise. Figure 5(b) gives the segmentation result and its region resulting from Bayesian updating framework. The distance between the left and right boundary is assigned as the crack size. As a comparison, for a 20 *mm* crack, the crack length estimated from the *k*-means clustering[27] based segmentation is 30 *mm*, while the estimated crack size obtained from Bayesian updating algorithm is 25 *mm*, providing more accurate crack size estimation. Furthermore, the crack size estimated is larger than the true crack size, ensuring the conservative measure of the damage.

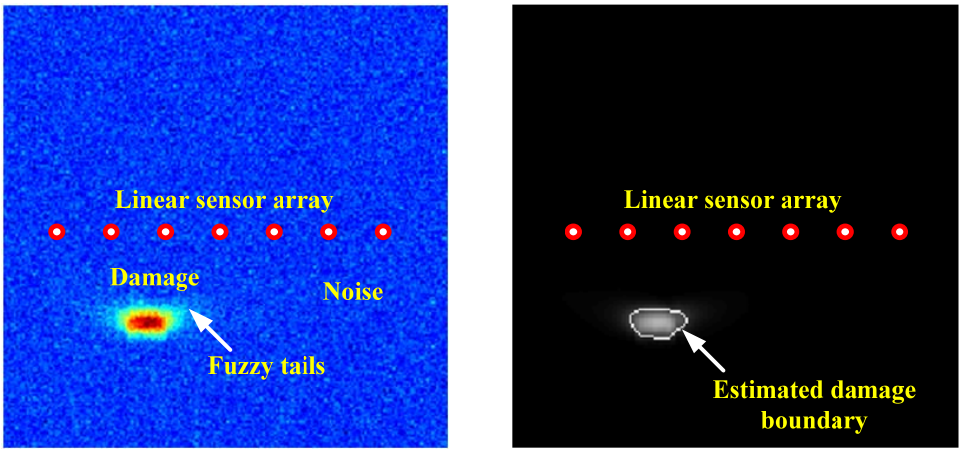


(a) (b)

Figure 5. (a) An image by *f-k* migration technique and (b) the Bayesian based segmentation result

*6.2 Validation at multiple locations*

Simulations are carried out at different crack locations to examine the accuracy and robustness of the Bayesian based image segmentation method. With the same simulation as in Figure 4, the coordinate of the crack centers are set as the **location** column in Table 1. The f-k migration imaging procedure is carried out for each crack, and then Bayesian based image segmentation is applied to extract the area of damage. The resulting crack lengths, given in Table 1 shows that the estimated crack sizes are very close to the true crack sizes, and the estimated crack location by the peak position of the 2-D distribution map is highly close to the true crack center location. Note that the spatial resolution of the resulting image of the two-dimensional damage distribution map is the mesh size of the simulation being 2.5*mm* in both horizontal and vertical directions.

Table 1 Center location and damage size for multi-location simulation (Unit: *mm*)

| Crack Index | True values | | Estimated values | |
|---|---|---|---|---|
| | Size | Location | Size | Location |
| d1 | 20 | (0,80) | 27.5 | (0,80) |
| d2 | 20 | (60,80) | 25 | (60,80) |
| d3 | 20 | (120,80) | 22.5 | (117.5,80) |
| d4 | 20 | (0,110) | 27.5 | (0,110) |
| d5 | 20 | (60,110) | 27.5 | (57.5,110) |
| d6 | 20 | (120,110) | 22.5 | (117.5,107.5) |
| d7 | 20 | (0,140) | 27.5 | (0,140) |
| d8 | 20 | (60,140) | 25 | (57.5,137.5) |
| d9 | 20 | (120,140) | 22.5 | (117.5,137.5) |
| d10 | 20 | (0,170) | 27.5 | (0,170) |
| d11 | 20 | (60,170) | 22.5 | (57.5,167.5) |
| d12 | 20 | (120,170) | 22.5 | (117.5,167.5) |

*6.3 Effects of prior information*

The essential idea of Bayesian image segmentation using MRF is by introducing the relationship described with Markov random field to eliminate noise and fizzy disturbance. The MRF affects the segmentation procedure through applying Gibbs potential as the prior in the Bayesian updating framework, thus the Gibbs potential $\beta$ plays an

important role of the segmentation procedure. It determines how strongly the neighboring pixels affect the labeling of the estimated pixels. With the original image as shown in Figure 6 (a), when $\beta = 0$, the Bayesian segmentation only uses the likelihood function, thus reducing to the *k*-means clustering based segmentation, which suffers from noise as shown in Figure 6(b). It is difficult to determine the crack length with such segmentation. With increasing $\beta$, the noise is suppressed, and the apparent damage area shrinks closer to the real damaged area, as shown in the Figure 6(c) and Figure 6(d). Results show that the segmentation does not change when $\beta$ varies from 0.5 to 100, which reflects the stability of the segmentation procedure. The reason for the convergence phenomenon is that the Gibbs potential provides plays only an adjustment role in the Bayesian updating procedure, but not a dominating role.

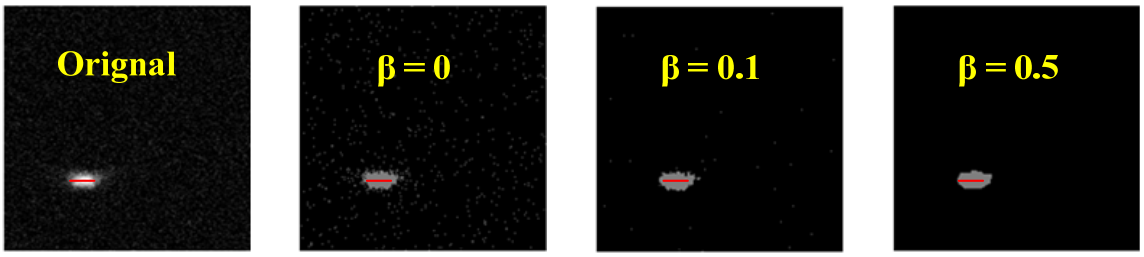


(a) (b) (c) (d)

Figure 6. Bayesian image segmentation with different Gibbs potentials

*6.4 Improvement with multiple-frequency excitation*

Reliable damage segmentation can be achieved by updating the segmentation with other priors such as the previous posterior distribution and damage imaging from different modalities. Different damage imaging techniques can be implemented for the same diagnosis task. Bayesian updating frame updates the segmentation continually, providing more reliable and accurate damage estimation. For the damage model simulated in the Section 6.1, the center frequency of excitation is 150 kHz. High frequency excitation yielding smaller wavelengths generates high resolution images, but with more fuzzy tails due to the complex modes of Lamb wave propagation. On the other hand, low frequency excitation generates low resolution but clear images.

The segmentation contains more information when a frequency range is applied for excitation rather than by one center frequency. It is more reliable for diagnosing a complex structure by choosing a frequency range as the excitation, because it is difficult to choose *a priori* the center frequency suited to the structure duo to its complex geometries and crack sizes. For the previous 20*mm* crack length case, the segmentation result for individual excitation center frequency being 150 *kHz* is 25*mm*. While the images generated from low frequencies the resolution can be low, the high frequencies generate fuzzy images. When Bayesian updating framework is used to update these images (with excitation frequencies, 50*kHz*, 100*kHz*, 150*kHz*, 200*kHz*, 250*kHz*, 300*kHz*) by taking the previous image intensity as a prior distribution, and the following detected image as a likelihood function one by one, and segmenting the posterior after all images are applied, the estimated crack size from the final segmentation is 22.5*mm*, which is closer to the true crack size than the result from a single excitation frequency of 150*kHz*.

## 7. Conclusions

A damage segmentation method in the context of structural health monitoring for sizing the damage is developed by taking advantage of prior information via Bayesian updating. Markov random field and its equivalent Gibbs random

field (GRF) are introduced as a prior to model the desired correlation between neighboring pixels. The migration technique is used for generating the raw image. The segmented damage region from the image obtained by segmentation has been demonstrated to be noise tolerant and the method is capable of providing accurate damage size estimation. The studies of Gibbs potential and damage at different locations show the stability of the damage segmentation method. The Bayesian based damage segmentation has the following merits:

(1) Spatial constraint using the neighboring pixel system is shown to be better than the *k*-means clustering based segmentation, which only considers the distance between the pixels and the clustering centers. As a result, the damage area is more focused by suppressing the fuzzy tails that often appear on both crack tips due to limited aperture covered by the sensors.

(2) The segmentation result gives damage shape and region estimation of the damaged area, discerning damaged regions from the background.

(3) More priors (e.g. multiple frequency excitations) can be easily introduced to enhance damage segmentation in the Bayesian updating framework.

**Acknowledgement**

The authors gratefully acknowledge the support of the research by the U.S. Air Force under Grant FA9550-07-1-0018 and by the NASA under Grant NNX08AC334.

**References**

[1] T. L. Anderson, *Fracture Mechanics: Fundamentals and Applications*, 3rd ed.: CRC Press, 2005.
[2] X. Lin and F. G. Yuan, "Damage Detection of a Plate Using Migration Technique," *Journal of Intelligent Material Systems and Structures,* vol. 12, pp. 469-482, 2001.
[3] X. Lin and F. G. Yuan, "Experimental Study Applying a Migration Technique in Structural Health Monitoring," *Structural Health Monitoring,* vol. 4, pp. 341-353, 2005.
[4] L. Wang and F. G. Yuan, "Damage Identification in a Composite Plate Using Prestack Reverse-Time Migration Technique," *Structural Health Monitoring,* vol. 4, pp. 195-211, 2005.
[5] X. Zhao, H. Gao, G. Zhang, B. Ayhan*, et al.*, "Active Health Monitoring of an Aircraft Wing with Embedded Piezoelectric Sensor/Actuator Network: I. Defect Detection, Localization and Growth Monitoring," *Smart Materials and Structures,* vol. 16, pp. 1208-1217, 2007.
[6] R. Sicard, J. Goyette, and D. Zellouf, "A Saft Algorithm for Lamb Wave Imaging of Isotropic Plate-Like Structures," *Ultrasonics,* vol. 39, pp. 487-494, 2002.
[7] W. Liu and J. W. Hong, "Three-Dimensional Lamb Wave Propagation Excited by a Phased Piezoelectric Array," *Smart Materials and Structures,* vol. 19, pp. 085002, 2010.
[8] C. H. Wang, J. T. Rose, and F. K. Chang, "A Synthetic Time-Reversal Imaging Method for Structural Health Monitoring," *Smart Materials and Structures,* vol. 13, pp. 415-423, 2004.
[9] J. A. Noble and D. Boukerroui, "Ultrasound Image Segmentation: A Survey," *IEEE Transactions on Medical Imaging,* vol. 25, pp. 987-1010, 2006.
[10] J. B. Ihn and F. K. Chang, "Pitch-Catch Active Sensing Methods in Structural Health Monitoring for Aircraft Structures," *Structural Health Monitoring,* vol. 7, pp. 5-19, 2008.
[11] J. E. Michaels, J. S. Hall, and T. E. Michaels, "Adaptive Imaging of Damage from Changes in Guided Wave Signals Recorded from Spatially Distributed Arrays," *SPIE Conference*, San Diego, CA, USA, 2009, pp. 729515-11.
[12] R. O. Duda, P. E. Hart, and D. G. Stork, *Pattern Classification*, 2nd ed. New York: Wiley, 2001.
[13] C. Carson, S. Belongie, H. Greenspan, and J. Malik, "Blobworld: Image Segmentation Using Expectation-Maximization and Its Application to Image Querying," *Pattern Analysis and Machine Intelligence, IEEE Transactions on,* vol. 24, pp. 1026-1038, 2002.
[14] G. Kuntimad and H. S. Ranganath, "Perfect Image Segmentation Using Pulse Coupled Neural Networks," *Neural Networks, IEEE Transactions on,* vol. 10, pp. 591-598, 1999.
[15] D. L. Pham and J. L. Prince, "An Adaptive Fuzzy C-Means Algorithm for Image Segmentation in the Presence of Intensity Inhomogeneities," *Pattern Recognition Letters,* vol. 20, pp. 57-68, 1999.

[16] C. A. Bouman and M. Shapiro, "A Multiscale Random Field Model for Bayesian Image Segmentation," *Image Processing, IEEE Transactions on,* vol. 3, pp. 162-177, 1994.
[17] S. D. Olabarriaga and A. W. M. Smeulders, "Interaction in the Segmentation of Medical Images: A Survey," *Medical image analysis,* vol. 5, pp. 127-142, 2001.
[18] K. Held, E. R. Kops, B. J. Krause, W. M. Wells, III*, et al.*, "Markov Random Field Segmentation of Brain Mr Images," *Medical Imaging, IEEE Transactions on,* vol. 16, pp. 878-886, 1997.
[19] S. Geman and D. Geman, "Stochastic Relaxation, Gibbs Distributions, and the Bayesian Restoration of Images," *Pattern Analysis and Machine Intelligence, IEEE Transactions on,* vol. PAMI-6, pp. 721-741, 1984.
[20] T. N. Pappas, "An Adaptive Clustering Algorithm for Image Segmentation," *IEEE transactions on signal processing,* vol. 40, pp. 901-914, 1992.
[21] A. H.-S. Ang and W. H. Tang, *Probability Concepts in Engineering Planning and Design*. New York: Wiley, 1975.
[22] G. Li, F. G. Yuan, R. Haftka, and N. H. Kim, "Bayesian Segmentation for Damage Image Using Mrf Prior," *SPIE Conference*, San Diego, CA, USA, 2009, pp. 72920J-12.
[23] Y. Zhang, M. Brady, and S. Smith, "Segmentation of Brain Mr Images through a Hidden Markov Random Field Model and the Expectation-Maximization Algorithm," *Medical Imaging, IEEE Transactions on,* vol. 20, pp. 45-57, 2001.
[24] J. Angulo and J. Serra, "Modelling and Segmentation of Colour Images in Polar Representations," *Image and Vision Computing,* vol. 25, pp. 475-495, 2007.
[25] S. Z. Li, *Markov Random Field Modeling in Image Analysis*, 3rd ed.: Springer, 2009.
[26] M. H. DeGroot, *Optimal Statistical Decisions*. New York,: McGraw-Hill, 1969.
[27] O. Demirkaya, M. H. Asyali, and P. K. Sahoo, *Image Processing with Matlab: Applications in Medicine and Biology*: CRC Press, 2008.